Eur. Phys. J. D **40**, 169–173 (2006)
DOI: 10.1140/epjd/e2006-00146-7

THE EUROPEAN PHYSICAL JOURNAL D

Radiative lifetimes of Zr III excited levels

R. Mayo[1], J. Campos[1], M. Ortiz[1], H. Xu[2], S. Svanberg[2], G. Malcheva[3], and K. Blagoev[3,a]

[1] Department of Atomic, Molecular and Nuclear Physics, Univ. Complutense de Madrid, 28040 Madrid, Spain
[2] Department of Physics, Lund Institute of Technology, PO Box 118, 221 00 Lund, Sweden
[3] Institute of Solid State Physics, 72 Tzarigradsko Chaussee, 1784 Sofia, Bulgaria

Received 16 February 2006
Published online 23 June 2006 –

Abstract. We report on radiative lifetimes of 4d5p excited states of Zr III produced in a laser produced plasma. The ions were populated either in the ground state or in metastable states, and the number of ions is strongly dependent on the application of an external magnetic field, which is shown to be very important when using the time-resolved laser-induced fluorescence technique for lifetime measurements in highly charged ions. The experimental lifetime results fall in the region 1–2 ns with statistical uncertainties less than 7%. The experimental values were compared with multi-configuration Hartree-Fock calculations showing an agreement within 12–20%. The experimental values are systematically higher than the theoretical ones.

PACS. 32.70.Cs Oscillator strengths, lifetimes, transition moments – 52.38.-r Laser-plasma interactions

1 Introduction

Experimental investigations of radiative lifetimes of excited levels of multiply charged ions are of substantial interest, because of the recent achievements in astrophysics and regarding high temperature plasma devices. As is pointed out in reference [1] the Zr II and Zr III spectra are of astrophysical interest. In particular, Zr III spectral lines were observed in the emission of the chemically peculiar B-type star χ-Lupi. In this paper we report the first radiative lifetime measurements of Zr III excited levels.

Experimental investigations of radiative lifetimes of excited levels of multiply ionized atoms are usually a subject of the beam-foil method. This is because the beam–foil method easily provides excited levels of ionized atoms, including multiply charged ones. The method has the possibility to study excited levels with short natural lifetimes ($\sim$1 ns); characteristic values for ionized atom excited levels. Potential problems of this method are spectral line blending caused by limited spectral resolution, and cascading effects, which sometimes may lead to considerable errors. The latter problem can be resolved by a full cascade analysis of the decay curves or by using the beam–laser modification of the method.

The time resolved laser induced fluorescence technique (TRLIF) is suited for measuring radiative lifetimes of excited levels in free atoms and ions since, it requires relatively simple equipment, compared to the beam-foil equipment, and at the same time provides accurate values. However, the TRLIF method is limited, when applied to highly ionized atoms (stages of ionization $\geq$2), because it is difficult to obtain a sufficient concentration in the ground and metastable ionic levels. However, a laser produced plasma can provide multiply ionized atoms allowing laser spectroscopic technique measurements (see, e.g., [2–4]). The source of the ions produces atoms and ions in different stages of ionization, in the ground or in excited levels. The latter ones, decaying radiatively, populate the ground or metastable levels of atoms and ions, which may then be used for excitation.

2 Previous work

The Zr III ground electronic configuration is [Kr]$4d^2$, and the $4d5s$, and $5s^2$ are the low-lying even-parity configurations, while $4d5p$ and $5s5p$ are low-lying odd-parity configurations.

A literature survey shows that there are only few investigations dedicated to the radiative constants of the Zr III spectrum, and in all of them only theoretical data for oscillator strengths and transition probabilities were obtained. The Cowan Multi-configurational Hartree-Fock (MHF) code was employed for calculating oscillator strengths of Zr III spectral lines in the spectral region 1190–3100 Å. The lines originate from the excited levels with energy $E_i \leq 13$ eV [5]. The relativistic multiconfigurational approximation taking core polarization into account was

[a] e-mail: kblagoev@issp.bas.bg

Table 1. Radiative lifetimes of Zr III excited levels (data in ns).

Level	E, cm^{-1}	Starting level	Starting level, cm^{-1}	λ_{exct} (nm)$_{air}$	λ_{obs} (nm)$_{air}$	Experiment This work	Theory This work	Theory [9]	Theory [5]
$4d5p\ z\ ^1\mathrm{D}^o_2$	53647.21	$4d^2\ ^1\mathrm{D}_2$	5741.5	208.68	286.9	1.76(5)	1.52	1.53	1.48
$4d5p\ z\ ^3\mathrm{D}^o_1$	55614.42	$4d^2\ ^3\mathrm{P}_0$	8062.0	210.23	268.6	1.08(7)	0.95	0.96	0.91
$4d5p\ z\ ^3\mathrm{D}^o_2$	56435.65	$4d^2\ ^3\mathrm{P}_1$	8325.6	207.79	265.6	1.15(4)	0.92	0.94	0.89
$4d5p\ z\ ^3\mathrm{D}^o_3$	57346.83	$4d^2\ ^3\mathrm{P}_2$	8838.2	206.08	264.4	1.05(5)	0.92	0.93	0.89
$4d5p\ z\ ^3\mathrm{F}^o_2$	55555.63	$4d^2\ ^3\mathrm{P}_1$	8325.6	211.66	269.0	1.90(10)	1.55	1.55	1.51

used to calculate the allowed $5s^2\ ^1\mathrm{S}_0 - 5s5p\ ^1\mathrm{P}_1$ and forbidden $5s^2\ ^1\mathrm{S}_0 - 5s5p\ ^3\mathrm{P}_1$ [6] transitions. Further papers in which oscillator strengths of Zr III spectral lines have been calculated are references [7,8]. In the most extensive paper [9], the Hartree–Fock method was employed for calculation of the oscillator strengths of a number of spectral lines. Relativistic quantum defect orbital method with and without core–valence correlations has been employed for calculating some of the $4d^2 - 4dns$, $4dnp$ and $4dnd$ oscillator strengths [10]. Very recently, some energy levels and transition probabilities pertaining to Zr III excited levels with $J = 0$, 1 have been calculated using the relativistic configuration interaction Dirac – Breit approach [11].

To our knowledge there are no papers on the determination of the radiative lifetimes of Zr III excited levels. In a previous paper [12] some of us measured transition probabilities of the $4d5p - 4d^2$, $4d5s$ and $4d5d - 4d5p$ transitions using the laser-induced break-down spectroscopy (LIBS) method. The experimental results were compared with theoretical data.

3 Experimental and theoretical lifetimes

The experimental set-up used in the present work has been described in details elsewhere (see, e.g., [2,13]). The Zr III ions were produced in a plasma by laser ablation using a pulsed Nd:YAG laser (Continuum Surelite), which had a pulse energy of up to 10 mJ. The impinging laser pulses produced the Zr plasma from a rotating Zr foil target in vacuum (10^{-5}–10^{-6} mbar) (Fig. 1). The levels under investigation were excited in a single-step process from the $4d^2\ ^1\mathrm{D}_2$, $4d^2\ ^3\mathrm{P}$ levels of the ground electron configuration $4d^2$, which have energies from 5741 cm^{-1} to 8838 cm^{-1}.

The excitation laser pulse, which was obtained from a Nd:YAG pumped dye laser (Continuum ND-60), had a short duration (about 1 ns), since the pumping laser pulses were compressed by using stimulated Brillouin scattering in water. To obtain the required excitation laser wavelengths, the third harmonic of the radiation from the dye laser, operating with DCM dye, was obtained using a KDP and a BBO crystal. The two lasers were synchronized by a pulse generator (Stanford Research Systems Model DG535) with the excitation laser pulse at a selected delay after the ablation. The third-harmonic beam passed horizontally through the plasma at a distance of 9 mm above the foil. The directions of the plasma-producing laser beam, excitation laser beam and observation were orthogonal. The fluorescence light was filtered by a 1/8 m monochromator (reciprocal linear dispersion 6.4 nm/mm), and then registered by a Hamamatsu R1564U multiplier tube (200 ps rise time). The signal was averaged and stored in a digital oscilloscope (Tektronix Model DSA 602). Table 1 presents the energy levels measured and the excitation schemes used.

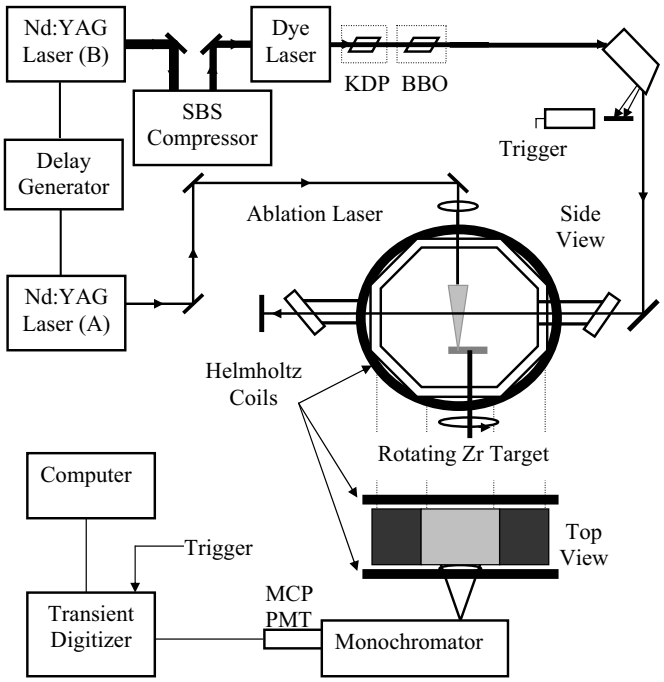

Fig. 1. Experimental set-up.

In connection with the work presented in reference [2] it was found that the application of a suitable magnetic field leads to a reduction of the background light, which is due to the recombination between the ions and the electrons in the plasma. The recombination decreases leads to an increase in concentration of ions in the ground term. The magnetic field was arranged perpendicular to the plasma producing laser beam and the induced ion flow, and parallel to the detection direction (Fig. 1). Lifetime measurements in multiply ionized atoms (Ce IV) were performed using the above technique [2].

As an example, Figure 2 illustrates the changes in the laser-induced fluorescence signal (peak 2) from the 53647.21 cm^{-1} level and the background due to

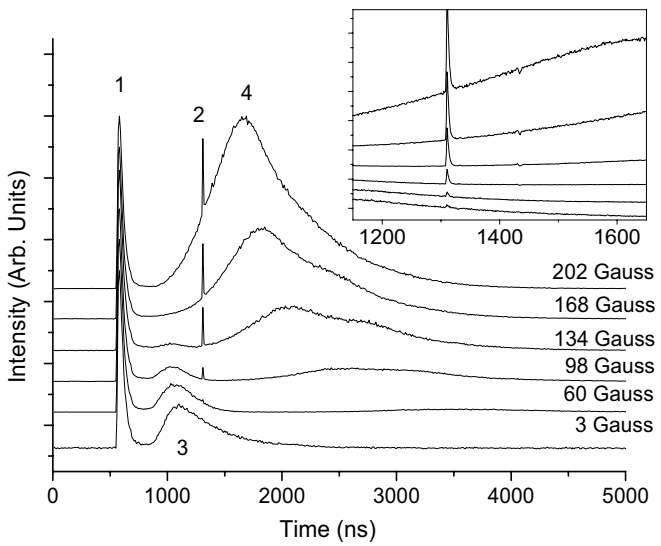

Fig. 2. Signals due to the 53647.21 cm^{-1} level and the background due to recombination light between the ions and electrons as a function of the time for different magnetic fields observed with monochromator set to 287 nm. Peak 1 corresponds to the total emission from the laser produced plasma; peak 2 – laser-induced fluorescence signal from 53647.21 cm^{-1} level; peak 3 – background light due to Zr III ion recombination; peak 4 – recombination light (see text).

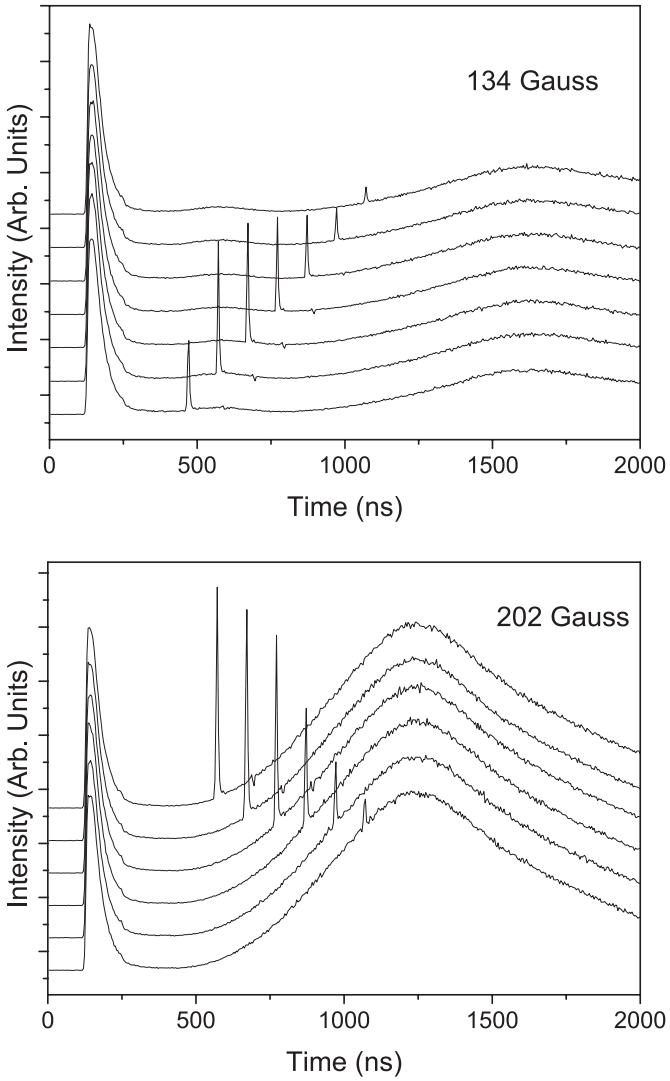

Fig. 3. The laser-induced fluorescence signal intensity from the 53647.21 cm^{-1} level as a function the delay time between the ablation and excitation pulses in the magnetic fields of 134 Gauss and 202 Gauss.

recombination light between ions and electrons in different magnetic fields. The peak 1, having a halfwidth of approximately 60 ns, is due to emission from excited levels of all species in the plasma. It can be seen from Figure 2 that the maximum 3 decreases when the magnetic field increases. This leads to the appearance and increase of the signal from the excitation of the 53647.21 cm^{-1} level of Zr III (peak 2). This fact leads to the conclusion that the maximum 3 is connected to the recombination involving Zr III ions. The inset in Figure 2 shows the same data for the time-resolved laser-induced fluorescence on a higher time resolution scale.

Figure 3 shows the variation of the laser-induced fluorescence signal (peak 2) as a function of delay time for two different magnetic field strengths.

Figures 2 and 3 can also be used to illustrate the variation of concentration of ions in the metastable level at 5741 cm^{-1} of the ground term of Zr III, since the fluorescence signal intensity is proportional to the population of the initial level. It can be supposed that in the magnetic field the electrons and ions are separated, which leads to the reduction of the recombination of ground term Zr III ions. The population becomes enough to realize excitation from it and observe fluorescence from the Zr III excited states. On the other hand, at larger magnetic fields the plasma volume reduces and the recombination of the Zr ions of different stage of ionization increases. This leads to the maximum 4 (Fig. 2). It can be seen from Figure 3 that the signal from the Zr III 53647.21 cm^{-1} level decreases and disappears when the delay of the excitation laser pulse is increased.

As can be seen from Figures 2 and 3, the recombination background can be reduced considerably by choosing an appropriate magnetic field when the time-resolved laser induced fluorescence signals were recorded at delay times in the range of 0.6 μs and 1.0 μs. The lifetime determined in the present work were measured at a typical magnetic field of 100 G. From data of the kind shown in Figure 2 we can make an estimation of the ion speed to study the flight-out-of-view effect. When the delay time is 0.8 μs, the velocity of the doubly ionized zirconium atoms having traveled 9 mm to the interaction volume with the excitation beam was about 11 km/s. For a 10 ns interval corresponding to 5 decay times for a level with a lifetime of 2 ns the ion flight distance is 110 μm along the vertical direction. This is much smaller than the diameter of

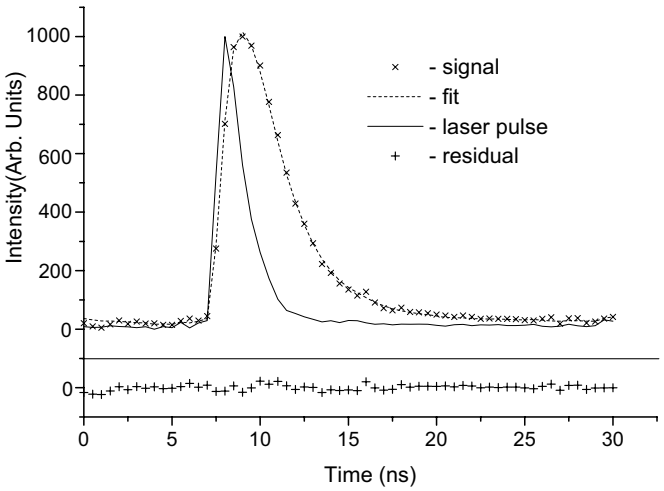

Fig. 4. A typical experimental time-resolved signal from the 53647.21 cm^{-1} level in Zr III. A recording of the laser pulse shape is also included. Residuals from the fitting curve and the experimental points are presented in the lower part of the figure.

the excitation beam. Moreover, the entrance slit of the monochromator was orientated along the ablation laser beam. Therefore, the flight-out-of-view effects will be negligible for measurements of such short lifetimes.

In order to obtain a sufficiently high signal-to-noise ratio every decay curve was obtained by averaging fluorescence photons from 1000 excitation pulses. For each lifetime measurement three recording were prepared: the excitation laser pulse, the fluorescence signal and the background. The temporal shape of laser pulses was recorded when the plasma producing laser beam was blocked. The time dependent background due to recombination light was recorded after the excitation laser pulses were blocked. The example of laser pulse and fluorescence curves is presented in Figure 4. Lifetime values were obtained by least-square fitting procedure of the laser-induced fluorescence curves to a convolution of the recorded laser pulse and a pure exponential function. When the measured lifetime is comparable with the laser pulse duration, the fluorescence intensity can be expressed as:

$$I(t) = C \int_{-\infty}^{t} P(t')E(t-t')dt \qquad (1)$$

where C is constant, $P(t')$ is the laser pulse shape, and $E(t)$ is the fluorescence decay curve for instantaneous excitation which is mathematically defined as $E(t) = 0$ for $t \leq 0$ and $E(t) = \exp(-t/\tau)$ for $t \geq 0$. This means that the real fluorescence curve is the convolution between the laser pulse shape and an exponential decay. Before the convolution procedure the nonlinear background was subtracted. In the convolution procedure the excitation laser pulse and fluorescence signal were normalized. Assuming Poisson statistics, the experimental points were weighed by $1/N_i$, where N_i is the number of counts in the ith channel of the digital oscilloscope. As can be seen from residual between the experimental curve and the fitted curve presented in the particular example in Figure 4, the difference between the points of experimental fluorescence and fitted curve did not exceed 2.3% of the maximum fluorescence value.

For each measured level, about 10–15 fluorescence decay curves were recorded under different experimental conditions. Parameters varied were the energy of the laser pulses, the value of the external magnetic field, the delay between the ablation and excitation pulses, and the high voltage supplied to the photomultiplier tube. Under the different experimental conditions, intensities of the detected fluorescence signals were changed by a factor of 3–6, and the evaluated lifetimes did still stay constant, which implied that there is no radiation trapping or other detrimental effect in the measurements. As an example, the change of signal intensity as a function of the delay time between the plasma generation and the excitation pulse can be clearly observed in Figure 3. In order to avoid saturation effects, the fluorescence signals were detected with different neutral density filters inserted in the exciting laser light path, an aspect important when a deconvolution is applied. The lifetime values and their errors presented in Table 1 were the result of averaging over the data of 10–15 decay curves. The error of each measurement did not exceed 5%. The error bars correspond to two standard deviations.

In Table 1 theoretical calculations of radiative lifetimes of the experimentally investigated excited $4d5p$ levels are also presented. The calculations were performed using the Cowan code [14], starting with LS coupling as an approximation for the basis electron configurations, which well represents the levels of interest [5]. In the calculations the even-parity electron configurations $4d^2$, $4d5s$, $5s^2$, $4d6s$, $4d5d$ and $6p^2$ were taken into account, and the odd-electron configurations $4d5p$, $5s5p$, $6p$, $4d6p$, $4d4f$ were considered. The integrals R_k, F_k, G_k and spin-orbit integral (ξ^k) were left at their *ab initio* values. The fitting of the calculated energies to the experimental ones was performed using excited state energies from reference [9]. In Table 1 other author's theoretical results are also presented. They are obtained from the calculated oscillator strengths [5,9], where all spectral lines of Zr III states of interest have been considered.

As can be seen from Table 1 the experimental data are close to the theoretical values, within 12–20%, but systematically higher. A possible reason could be radiation trapping, which, however, is improbable. The experimental values, which were obtained at different ion concentrations, were found to be constant. The concentration was changed either by variation of ablation laser pulse energies or by the delay between ablation and excitation laser pulses.

In conclusion, in this paper the first experimental data for radiative lifetimes of levels belonging to the Zr III ion are reported. They agree reasonably well with theoretical values. The method of using a laser produced plasma in an applied magnetic field, with the effect of reducing the recombination of multicharged ions and therefore increasing

the ion concentration, was shown to be very promising for laser-induced fluorescence measurements of radiative lifetimes of excited levels in multicharged ions.

This work was supported by the EC under the program "Access to Research Infrastructures" under the grant RII3-CT-2003-506350, and the Bulgarian National Science Fond (contract 1516/05).

References

1. D.C. Morton, Astrophys. J. Suppl. Ser. **130**, 403 (2000)
2. Z.G. Zhang, S. Svanberg, P. Quinet, P. Palmeri, E. Biémont, Phys. Rev. Lett. **87**, 273001 (2001)
3. E. Biémont, H.P. Garnir, P. Palmeri, P. Quinet, Z.S. Li, Z.G. Zhang, S. Svanberg, Phys. Rev. A **64**, 022503 (2001)
4. E. Biémont, H.P. Garnir, P. Quinet, S. Svanberg, Z.G. Zhang, Phys. Rev. A **65**, 052502 (2002)
5. A. Redfors, Astronomy & Astrophysics **249**, 589 (1991)
6. J. Migdalek, M. Stanek, Z. Phys. D **27**, 9 (1993)
7. P.J. Malloy, S.J. Czyzak, Astrophys. Space Sci. **58**, 365 (1978)
8. K.D. Sen, A. Puri, Chem. Phys. Lett. **156**, 505 (1989)
9. J. Reader, N. Acquista, Phys. Scripta **55**, 310 (1997)
10. E. Charro, J.L. Lopez-Ayuso, I. Martin, J. Phys. B: At. Moll Phys. **32**, 4555 (1999)
11. D.R. Beck, L. Pan, Phys. Scripta **69**, 91 (2004)
12. R. Mayo, M. Ortiz, J. Campos, J. Quant. Spectr. Rad. Transfer **94**, 109 (2005)
13. H.L. Xu, A. Persson, S. Svanberg, K. Blagoev, G. Malcheva, V. Pentchev, E. Biémont, J. Campos, M. Ortiz, R. Mayo, Phys. Rev. A **70**, 042508 (2004)
14. R.D. Cowan, *The Theory of Atomic Structure and Spectra* (Berkeley, University of California Press 1981)